Langmuir

ARTICLE

pubs.acs.org/Langmuir

Substrate-, Wavelength-, and Time-Dependent Plasmon-Assisted Surface Catalysis Reaction of 4-Nitrobenzenethiol Dimerizing to *p,p′*-Dimercaptoazobenzene on Au, Ag, and Cu Films

Bin Dong,[†,‡] Yurui Fang,[†] Xiaowei Chen,[§] Hongxing Xu,[†,∥] and Mengtao Sun*[,†]

[†]Beijing National Laboratory for Condensed Matter Physics, Institute of Physics, Chinese Academy of Sciences, P.O. Box 603-146, Beijing 100190, PR China

[‡]School of Science, Dalian Nationalities University, Dalian 116600, PR China

[§]Departamento de Ciencia de los Materiales, Ingeniería Metalúrgica y Química Inorgánica, Facultadde Ciencias, Universidad de Cádiz (Campus Río San Pedro), E-11510 Puerto Real, Cádiz, Spain

[∥]Division of Solid State Physics, Lund University, Lund 22100, Sweden

ABSTRACT: In this article, we experimentally investigate the substrate, wavelength, and time dependence of the plasmon-assisted surface-catalyzed dimerization of 4-nitrobenzenethiol to form *p,p′*-dimercaptoazobenzene on Au, Ag, and Cu films. We provide direct experimental evidence that surface plasmon resonance plays the most important role in these surface-catalyzed reactions. It is found that the reaction is strongly dependent on the substrate, the wavelength of the laser, and the reaction timescales. Our experimental results revealed that optimal experimental conditions can be rationally chosen to control (accelerate or restrain) this reaction. The experimental results are also confirmed by theoretical calculations.

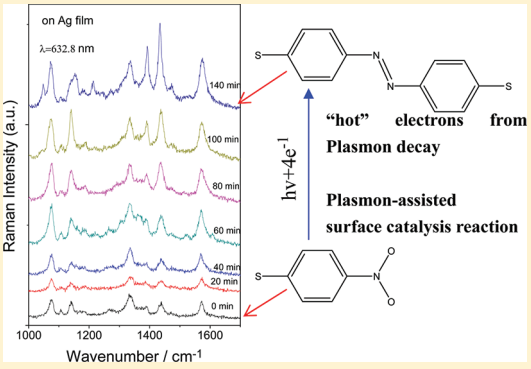

I. INTRODUCTION

Nanoscale chemical reaction control is expected to play an important role in both surface photochemical reactions and building complicated molecular device structures. Recently, an electric-current-induced chemical reaction was successfully realized with scanning tunneling microscope (STM) probes on a conductive surface.[1] Furthermore, STM control of a chemical reaction for single-molecule synthesis has been reviewed.[2] However, on non-conductive surfaces, a photochemical approach with a near-field scanning optical microscope (NSOM) has been employed.[3] Local-field-enhanced surface photochemical reactions on surface-supported metallic particles have been observed.[4] Very recently, the nanoscale control of reversible chemical reactions, namely, polymerization and depolymerization between C_{60} molecules, was investigated experimentally by negative and positive bias voltage values.[5] Rate-determining factors in the chain polymerization of molecules initiated by local single-molecule excitation were also reported.[6] Recent experimental work has also demonstrated that chemical bonds can be selectively broken or formed by the tunneling electron current.[7−9] The surface-catalyzed formation of *p,p′*-dimercaptoazobenzene (DMAB) by the oxidation of 4-aminothiophenol (PATP) or the reduction of 4-nitrobenzenethiolate (4NBT) has been reported experimentally and theoretically.[10−18] Remote excitation surface-enhanced Raman scattering (SERS) spectra by a plasmonic waveguide[19,20] further indicated the oxidation of PATP and the reduction of 4NBT to DMAB induced by surface plasmon resonance. Additional reports demonstrate how to control the surface-catalyzed oxidation of PATP to DMAB by different pH values on different substrates.[15−17] However, how to control (accelerate or restrain) the surface-photocatalyzed reduction of 4NBT to DMAB experimentally by different experimental factors, such as the substrate, wavelength, and reaction timescales, is still not clear.

In this article, we attempt to control the surface-catalyzed reduction of 4NBT to DMAB experimentally using different substrates, laser wavelengths, and timescales. First, Au, Ag, and Cu films were prepared using the vacuum electron beam evaporator. Second, the surface-catalyzed reduction of 4NBT reduced to DMAB was measured under different experimental conditions using SERS spectroscopy. Third, the conclusion was derived that optimal experimental conditions can be rationally chosen to control (accelerate or restrain) this reaction. Finally, theoretical calculations strongly supported the experimental results.

II. EXPERIMENTAL SECTION

The substrates for SERS measurement were prepared by evaporating Au, Ag, and Cu metal onto silicon under high vacuum using a vacuum

Received: May 18, 2011
Revised: July 30, 2011
Published: August 05, 2011

dx.doi.org/10.1021/la2018538 | *Langmuir* 2011, 27, 10677–10682

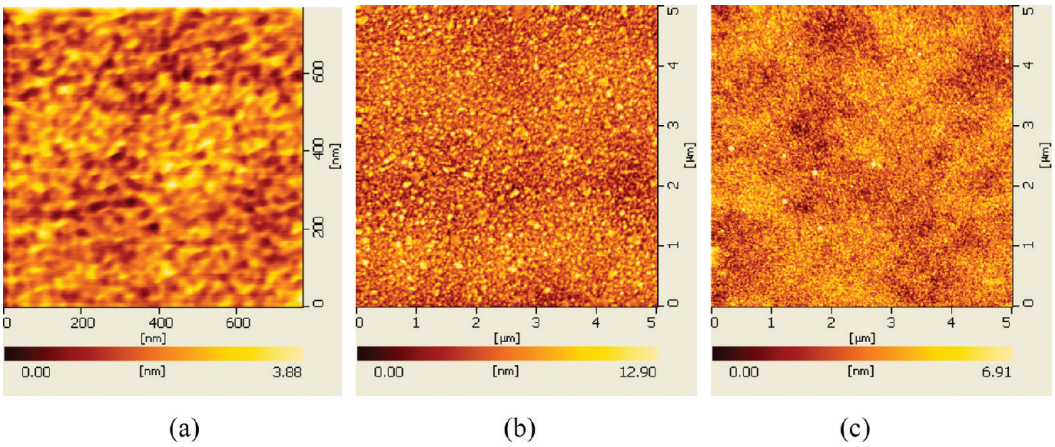

Figure 1. AFM images of the (a) Au, (b) Ag, and (c) Cu films.

electron beam evaporator (Peva-600E). The evaporation conditions were carefully controlled to produce a layer of different metals with an average thickness of 50 nm. The surface roughness was evaluated with atomic force microscopy (AFM, model SPA400). The AFM images (Figure 1a−c) show the surface of the substrate with different metals, and the average roughness (rms) values are 0.56, 2.03, and 1.04 nm for Au, Ag, and Cu films, respectively. The surface morphologies of Au, Ag, and Cu films were characterized by SEM (Hitachi S-4800). Figure 2a−c shows SEM images of these metal films. The Ag colloid was prepared by the citrate reduction of $AgNO_3$ as described by Lee et al.[21] The SEM imaging (Figure 2d) shows that the average diameter of the nanoparticles is about 110 nm. The SERS-active Au colloid was synthesized using the method of McFarland et al., and the average diameter of the nanoparticle is 25 nm.

The Au, Ag, and Cu films were immersed in a 1×10^{-5} M solution of 4NBT in ethanol for more than 5 h. The films were then sequentially washed with acetone, ethanol, and deionized water for 3 min, respectively. After these films were dried with N_2 gas, Ag nanoparticles were dropped on these films to create hot spots between the nanoparticles and these films. This method to make a nanoparticle−molecule−film junction can greatly enhance the Raman intensities.[13] The Raman spectra of 4NBT on Au, Ag, and Cu films were measured with a Renishaw inVia Raman system equipped with an integral microscope (Leica, DMLM). Lasers with wavelengths of 632.8 and 514.5 nm were used as the excitation sources. In our Raman experiment, the laser power irradiating the SERS sample was measured at 2 mW with a 100× objective. The appropriate holographic notch filter was placed in the spectrometer, and the holographic grating (1800 grooves/mm) and slit installed in the spectrometer produced a spectral resolution of 1 cm^{-1} with a repeatability of $\leq \pm 0.2$ cm^{-1}. Raman scattering was detected using a Peltier-cooled CCD detector (576 pixels × 384 pixels). The data acquisition time used in the experiment was 17 s for one spectrum.

III. THEORETICAL

To study the local surface plasmon resonance effect on SERS, the near-field distribution of the electromagnetic field was investigated with the finite difference time domain (FDTD) method[23] using FDTD Solutions software.[24] The electromagnetic field distribution of the system of Ag nanoparticles (diameter 110 nm) on the Au, Ag, and Cu films (thickness 50 nm) with a nanogap of 2 nm between Ag nanoparticles was calculated at incident light wavelengths of 514.5 and 632.8 nm, respectively. The permittivity of Au, Cu, and Ag was taken from the work of Palic.[25]

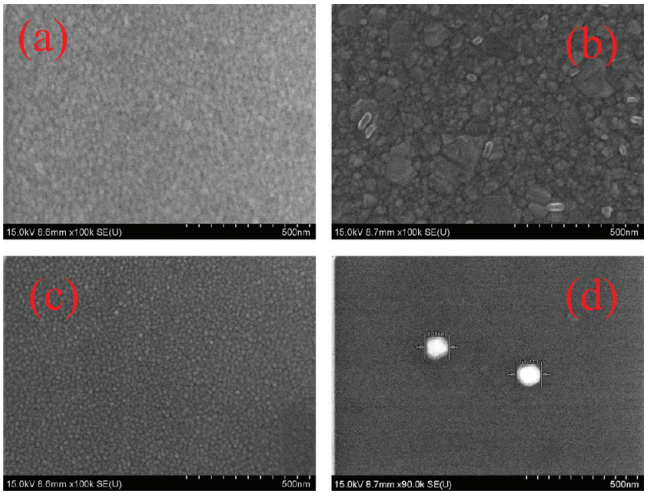

Figure 2. SEM images of the (a) Au, (b) Ag, and (c) Cu films and (d) Ag nanoparticles.

IV. RESULTS AND DISCUSSION

As we previously reported,[18] direct experimental evidence for the surface-catalyzed dimerization of 4NBT to form DMAB is the disappearance of Raman intensity at 1331 cm^{-1} ($\nu_s(NO_2)$ of 4NBT, see Figure 1 in ref 18) and the appearances of Raman intensity at around 1387 and 1432 cm^{-1} (ag_{16} and ag_{17} vibrational modes, respectively, related to −N═N− of DMAB, see Figure 1f in ref 18). We intended to follow the evolution of SERS intensities of these three vibrational modes on Au, Ag, and Cu films under irradiation with 514.5 and 632.8 nm lasers at different reaction timescales in this work.

Figure 3a demonstrates that the SERS intensities and profiles of a molecule adsorbed on the Cu film at an incident wavelength of 632.8 nm are nearly unchanged with different reaction times of up to more than 2 h, and the main Raman peak can be attributed to $\nu_s(NO_2)$ of 4NBT. Thus, the surface-catalyzed reduction of 4NBT to form DMAB does not occur in this case. In contrast, SERS intensities and profiles of molecules adsorbed on the Cu film are changed dramatically when the incident light is changed to 514.5 nm (Figure 3b), where the Raman intensity of $\nu_s(NO_2)$ of 4NBT disappears within 2 min and the Raman intensities of the ag_{16} and ag_{17} vibrational modes (related to −N═N− of DMAB)

dx.doi.org/10.1021/la2018538 |*Langmuir* 2011, 27, 10677–10682

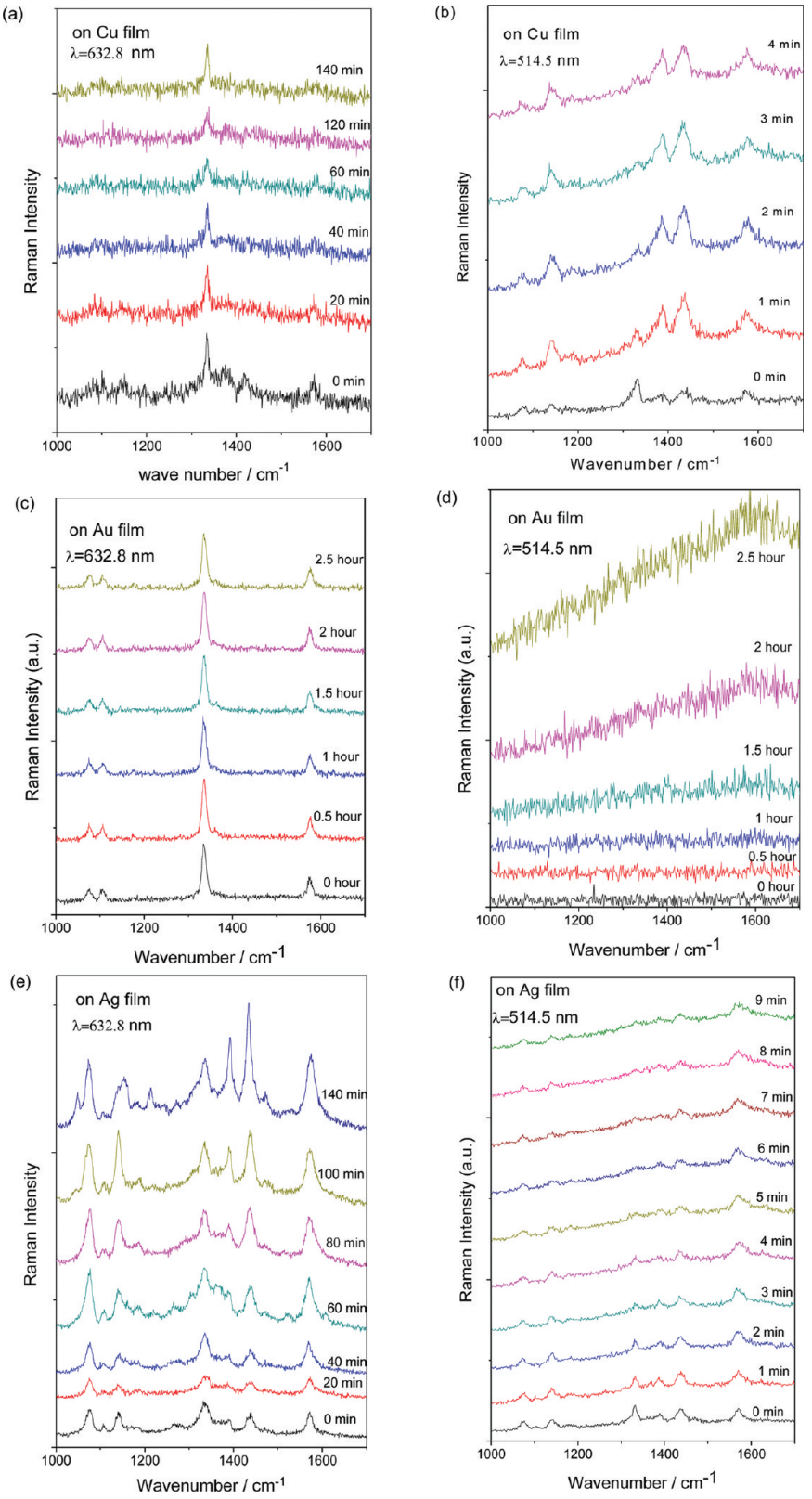

Figure 3. SERS spectra of 4NBT at the junction of a Ag nanoparticle on the Cu, Au, and Ag films system. (a, b) On the Cu film at incident wavelengths of 632.8 and 514.5 nm, respectively, (c, d) on the Au film at incident wavelengths of 632.8 and 514.5 nm, respectively, and (e, f) on the Ag film at incident wavelengths of 632.8 and 514.5 nm, respectively.

appear within 1 min. Therefore, 4NBT is rapidly converted to DMAB on the Cu film under these conditions. The wavelength-dependent surface-catalyzed reaction indicates that the potential barrier (V_{pb}) of this reaction should be $V_{pb} > 1.959$ eV on the Cu

dx.doi.org/10.1021/la2018538 |*Langmuir* 2011, 27, 10677–10682

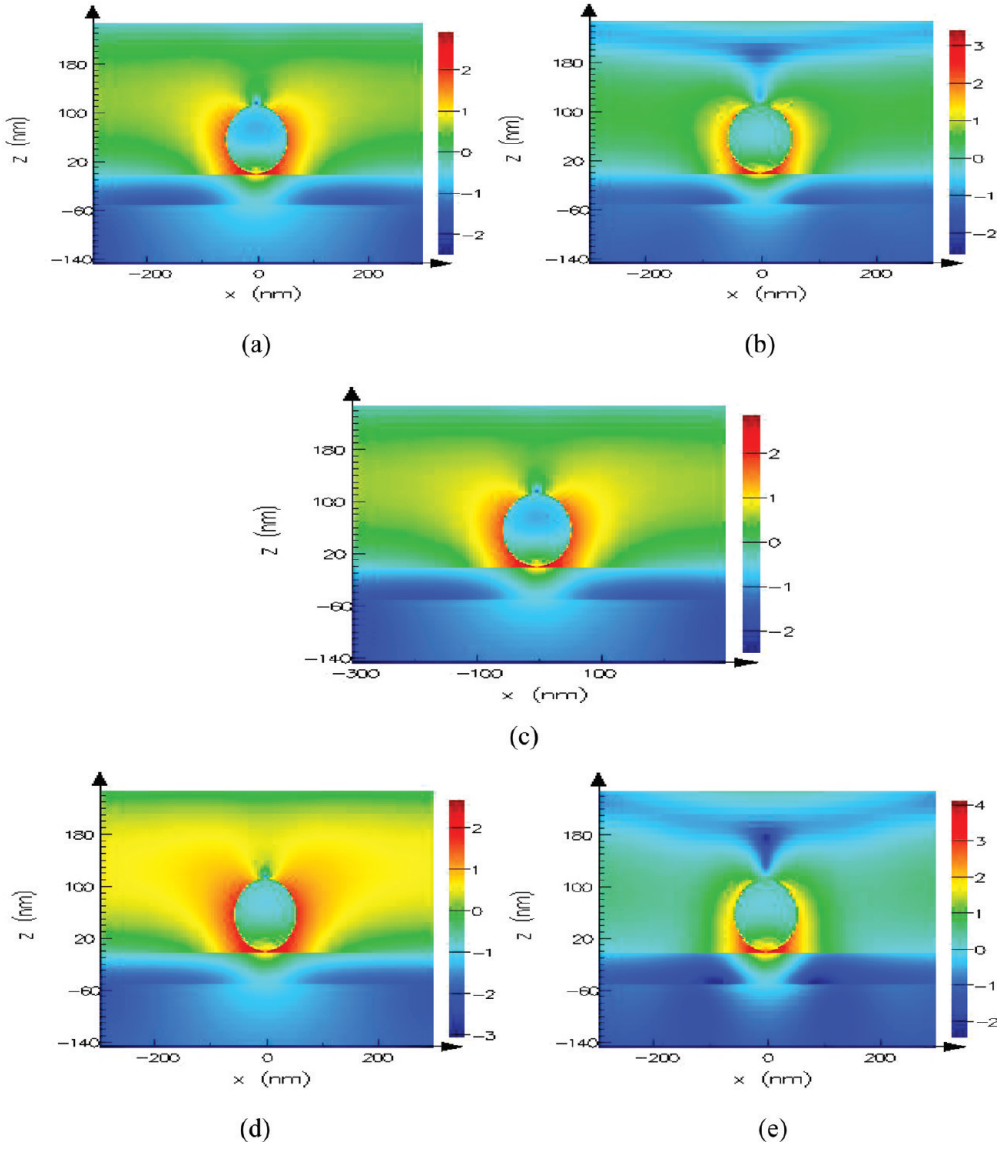

Figure 4. Local electric field distribution of (a, b) the Ag nanoparticle−Cu film at incident wavelengths of 632.8 and 514.5 nm, respectively, (c) the Ag nanoparticle−Au film at an incident wavelength of 632.8 nm, and (d, e) the Ag nanoparticle−Ag film at incident wavelengths of 632.8 and 514.5 nm, respectively, where the diameter of the Ag nanoparticle is 110 nm and the thickness of the Cu, Au, and Ag films is 50 nm. The electric field intensity distribution was simulated and plotted on a logarithmic scale.

film because the reaction does not take place when the wavelength of light is 632.8 nm (1.959 eV).

The calculated results, using FDTD, exhibited that the electromagnetic enhancement $|M|^2$ in the junction between a Ag nanoparticle and the Cu film at an incident wavelengths of 514.5 nm is much stronger than that at the incident wavelength of 632.8 nm (6.4×10^6 vs 6.8×10^5), where $|M| = |E_{local}/E_{in}|$, and E_{local} and E_{in} are the local and incident electric fields, respectively. Figure 4a,b shows the local electric field distribution of the Ag nanoparticle−Cu film at incident wavelengths of 632.8 and 514.5 nm, respectively.

To check whether the catalyzed reaction is dependent on the surface plasmon resonance or only on the interaction between a molecule and film without the surface plasmon, we also measured the first SERS spectrum of 4NBT, when 4NBT adsorbed on a Cu film 10 min later (line b (black line) in Figure 5). As shown in Figure 3b, the catalyzed reaction is complete within 2 min when the incident wavelength is 514.5 nm. Assuming that the catalyzed reaction is dependent on only the interaction between a molecule and film without the contribution of the surface plasmon, we measure the SERS spectrum when 4NBT adsorbed on the Cu film 10 min later. The measured SERS spectrum should show that the Raman intensity of $\nu_s(NO_2)$ of 4NBT at 1331 cm^{-1} disappears and the Raman intensities at around 1387 and 1432 cm^{-1} are strongly enhanced, which would confirm the occurrence of the catalyzed reaction. In fact, line b (black line) in Figure 5 shows that the Raman intensity of $\nu_s(NO_2)$ of 4NBT at 1331 cm^{-1} is the strongest peak, which confirmed that the catalyzed reaction did not occur without a surface plasmon, though the time of interaction between 4NBT and the Cu film (10 min) is longer than the catalyzed reaction time (2 min) in Figure 3b. This experiment provides experimental evidence confirming the important role of the surface plasmon in the surface-catalyzed reaction.

dx.doi.org/10.1021/la2018538 |*Langmuir* 2011, 27, 10677–10682

Figure 3c shows that 4NBT cannot be reduced to DMAB for up to 2.5 h with an incident wavelength of 632.8 nm on the Au film because the Raman intensity of $\nu_s(NO_2)$ of 4NBT is unchanged. Figure 4c is the local electric field distribution of the Ag nanoparticle−Au film at an incident wavelength of 632.8 nm. Figure 3d shows that there is almost no Raman profile up to 2.5 h later, which suggests that the Au film is not a good substrate at the incident wavelength of 514.5 nm because the coupling between conduction electrons and interband electronic transitions by using 514.5 nm light depresses the quality of the surface plasmon resonance of gold metals considerably.

We further studied the effects of the laser wavelength and timescale on the surface-catalyzed reaction of molecules adsorbed on the Ag film. At an incident wavelength of 632.8 nm, Figure 3e reveals that the Raman intensities of the ag_{16} and ag_{17} vibrational modes are much weaker than that of $\nu_s(NO_2)$ of 4NBT within 60 min. With the increase in reaction time (time of laser radiation), the Raman intensities of the ag_{16} and ag_{17} vibrational modes increase gradually. After 80 min of reaction, the Raman intensities of the ag_{16} and ag_{17} vibrational modes are gradually stronger than that of $\nu_s(NO_2)$ of 4NBT. After 140 min of reaction, the Raman intensities of the ag_{16} and ag_{17} vibrational modes become significantly stronger than that of $\nu_s(NO_2)$ of 4NBT. At an incident wavelength of 514.5 nm, the timescale of the reaction is much shorter than that at the incident wavelength of 632.8 nm (Figure 3f), which is completed within 5 min. The calculated results, using FDTD, indicate that the electromagnetic enhancements in the junction between a Ag nanoparticle and the Ag film at an incident wavelength of 514.5 nm is much stronger than that at 632.8 nm (1.7×10^8 vs 2.1×10^5). For this reason, the stronger electromagnetic field enhancement provided by the local surface plasmon can significantly shorten the reaction time. Figure 4d,e shows the local electric field distributions of the Ag nanoparticle−Ag film at incident wavelengths of 632.8 and 514.5 nm, respectively.

We propose the following mechanism for how the surface-catalyzed reaction takes place in converting 4NBT to DMAB (Scheme 1). The required $4e^{-1}$ are proposed to be "hot" electrons arising from the surface plasmon.[26−28] The light quanta stored in the plasmons can be reemitted as light, but some of the plasmons can also decay into two charge carriers, an electron and a "hole." It has been known for some time that plasmon decay can create hot electrons that have high kinetic energy, which can presumably drive the surface-catalyzed reaction.

It is worth emphasizing that the surface-catalyzed reduction of 4NBT to DMAB on Au and Cu films cannot be observed from time-dependent SERS spectra at an incident wavelength of 632.8 nm. However, at the same incident wavelength such a surface catalysis reaction occurs in Au sols (Figure 6) and in Cu sols (Figure 1f in ref 15). The reasons are that the specific surface areas of Au nanoparticles and Cu microparticles are much higher than those of Au and Cu films and there are more hot sites among nanoparticles than the single hot site in the nanoparticle−molecule−Au film junction. The electromagnetic enhancement $|M|^2$ in the nanogap of the nanoparticle−molecule−Au film junction is only 5.1×10^5. Figure 4c is the local electric field distribution of the Ag nanoparticle−Au film at an incident wavelength of 632.8 nm. It should be noted that the k of the electric field is perpendicular to the surface and the objective collecting the Raman signal is also perpendicular to the surface, so the effective electromagnetic enhancement in collecting SERS signals is weaker. It has been reported that the best angle between k and the surface for collecting Raman signals is 60° in tip-enhanced Raman scattering (TERS).[29] At an incident wavelength of 632.8 nm, our previous experimental study also certified that PATP in the Ag nanoparticle−molecule−Au film junction cannot be oxidized to DMAB (Figure 3d in ref 13) whereas PATP can be dimerized to DMAB

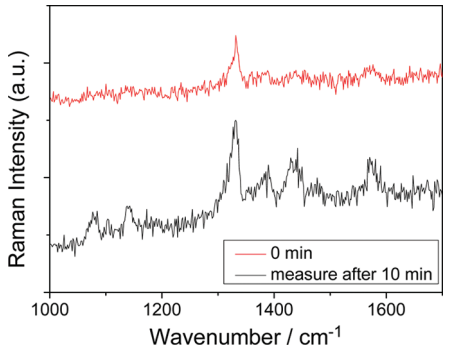

Figure 5. SERS spectra of 4NBT adsorbed on the Cu film. The top line (red) was measured when 4NBT adsorbed on the Cu film intermediately, and the bottom line (black) was measured for the first time when 4NBT adsorbed on the Cu film 10 min later.

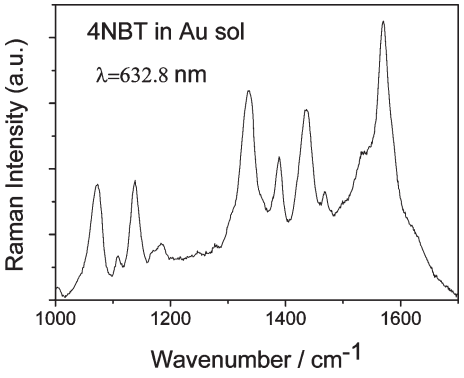

Figure 6. SERS spectra of 4NBT in a Au sol at an incident wavelength of 632.8 nm.

Scheme 1. Mechanism of the Plasmon-Assisted Surface-Catalyzed Reaction

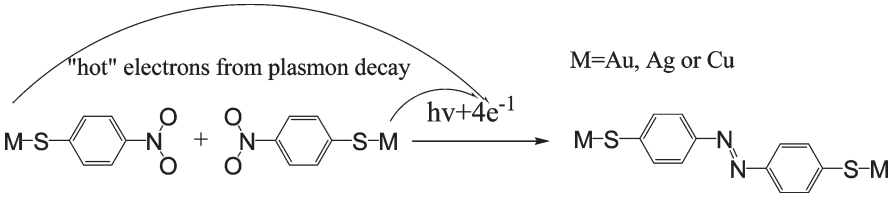

dx.doi.org/10.1021/la2018538 |Langmuir 2011, 27, 10677–10682

in the Au sol by the surface catalysis reaction in Figure 1e of ref 18. We noted that Liu and co-workers reported[30] that Raman intensities at 1387 and 1432 cm^{-1} were also dependent on the laser power.

V. CONCLUSIONS

The substrate-, wavelength-, and time-dependent surface catalysis reaction of DMAB produced from 4NBT by surface plasmon resonance on Au, Ag, and Cu films has been investigated. It is found that such a surface-catalyzed reaction can be rationally controlled (accelerated or restrained). It is a very important complement to our previous experimental study that DMAB can be produced from PATP because PATP and 4NBT are converted to DMAB by oxidation and reduction reactions, respectively. We also noted that such a surface catalysis reaction in colloids is much easier to conduct than that on films. Surface plasmon resonance plays the most important role in these surface-catalyzed reactions, and the hot electrons that decay from the plasmon cause the surface-catalyzed reaction.

AUTHOR INFORMATION

Corresponding Author
*E-mail: mtsun@aphy.iphy.ac.cn.

ACKNOWLEDGMENT

We thank Prof. Naomi J. Halas for suggestions on the measurements in Figure 5. This work was supported by the National Natural Science Foundation of China (grants 10874234, 90923003, 10804015, and 20703064) and the National Basic Research Project of China (grants 2009CB930701 and 2007CB936804). X.C. thanks the Ramón y Cajal program from the Ministry of Science and Innovation in Spain.

REFERENCES

(1) Okawa, Y.; Aono, M *Nature* **2001**, *409*, 683.
(2) Hla, S. W.; Rieder, K. H. *Annu. Rev. Phys. Chem.* **2003**, *54*, 307.
(3) Betzig, E.; Trautman, J. K *Science* **1992**, *257*, 189.
(4) Chen, C. J.; Osgood, R. M. *Phys. Rev. Lett.* **1983**, *50*, 1705.
(5) Nakaya, M.; Kuwahara, Y.; Aono, M.; Nakayama, T. *J. Nanosci. Nanotechnol.* **2011**, *11*, 2829.
(6) Mandal, S. K.; Okawa, Y.; Hasegawa, T.; Aono, M. *ACS Nano* **2011**, *5*, 2779.
(7) Stipe, B. C.; Rezaei, M. A.; Ho, W.; Gao, S.; Persson, M.; Lundqvist, B. I. *Phys. Rev. Lett.* **1997**, *78*, 4410.
(8) Lauhon, L. J.; Ho, W. *Phys. Rev. Lett.* **2000**, *84*, 1527.
(9) Lee, H. J.; Ho, W. *Science* **1999**, *286*, 1719.
(10) Wu, D. Y.; Liu, X. M.; Huang, Y. F.; Ren, B.; Xu, X.; Tian, Z. Q. *J. Phys. Chem. C* **2009**, *113*, 18212.
(11) Fang, Y. R.; Li, Y. Z.; Xu, H. X.; Sun, M. T. *Langmuir* **2010**, *26*, 7737.
(12) Huang, Y. F.; Zhu, H. P.; Liu, G. K.; Wu, D. Y.; Ren, B.; Tian, Z. Q. *J. Am. Chem. Soc.* **2010**, *132*, 9244.
(13) Huang, Y. Z.; Fang, Y. R.; Yang, Z. L.; Sun, M. T. *J. Phys. Chem. C* **2010**, *114*, 18263.
(14) Canpean, V.; Iosin, M.; Astilean, S. *Chem. Phys. Lett.* **2010**, *500*, 277.
(15) Sun, M. T.; Huang, Y. Z.; Xia, L. X.; Chen, X. W; Xu, H. X. *J. Phys. Chem. C* **2011**, *115*, 9629.
(16) Zong, S.; Wang, Z.; Yang, J.; Cui, Y. P. *Anal. Chem.* **2011**, *83*, 4178.
(17) Gabudean, A. M.; Biro, D.; Astilean, S. *J. Mol. Struct.* **2011**, *993*, 420.
(18) Dong, B.; Fang, Y. R.; Xia, L. X.; Xu, H.; Sun, M. T. *J. Raman Spectrosc.* **2011**, *42*, 1205.
(19) Sun, M. T.; Hou, Y. X.; Li, Z. P.; Liu, L. W.; Xu, H. X. *Plasmonics* **2011**, DOI: 10.1007/s11468-011-9251-2.
(20) Sun, M. T.; Hou, Y. X.; Li, Z. P.; Liu, L. W.; Xu, H. X. Submitted for publication.
(21) Lee, P. C.; Meisel, D. *J. Phys. Chem.* **1982**, *86*, 3391.
(22) McFarland, A. D.; Haynes, C. L.; Mirkin, C. A.; Van Duyne, R. P.; Godwin, H. A. *J. Chem. Educ.* **2004**, *81*, 544A.
(23) Kunz, K. S.; Luebber, R. J. *The Finite Difference Time Domain Method for Electromagnetics*; CRC Press: Cleveland, OH, 1993.
(24) *FDTD Solutions*, version 7.5; Lumerical Solutions, Inc.: Vancouver, BC, Canada, 2011.
(25) Palik, E. D. *Handbook of Optical Constants of Solids*; Academic Press: New York, 1985.
(26) Knight, M. W.; Sobhani, H.; Nordlander, P.; Halas, N. J. *Science* **2011**, *332*, 702.
(27) Moskovits, M. *Science* **2011**, *332*, 676.
(28) Shalaev, V. M.; Douketis, C.; Stuckless, J. T.; Moskovits, M. *Phys. Rev. B* **1996**, *53*, 11388.
(29) Sun, M. T.; Fang, Y.; Yang, Z.; Xu, H. X. *Phys. Chem. Chem. Phys.* **2009**, *11*, 9412.
(30) Liu, G. K.; Hu, J.; Zheng, P. C.; Shen, G. L.; Jiang, J. H.; Yu, R. Q.; Cui, Y.; Ren, B. *J. Phys. Chem. C* **2008**, *112*, 6499.